ELSEVIER

Coordination Chemistry Reviews
190–192 (1999) 1023–1047

COORDINATION CHEMISTRY REVIEWS

www.elsevier.com/locate/ccr

Molecules to build solids: high T_C molecule-based magnets by design and recent revival of cyano complexes chemistry

Michel Verdaguer [a,*], A. Bleuzen [a], V. Marvaud [a], J. Vaissermann [a], M. Seuleiman [a], C. Desplanches [a], A. Scuiller [a], C. Train [a], R. Garde [a], G. Gelly [a], C. Lomenech [a], I. Rosenman [b], P. Veillet [c], C. Cartier [a,d], F. Villain [a,d]

[a] *Laboratoire de chimie inorganique et matériaux moléculaires, Unité Associée au CNRS 7071, Case 42, Université Pierre et Marie Curie, 75252 Paris Cedex 05, France*
[b] *Groupe de physique des solides, Université Denis Diderot, Paris, France*
[c] *Institut d'Electronique Fondamentale, Université Paris-Sud, Orsay, France*
[d] *LURE, Université Paris-Sud, Orsay, France*

Contents

* Corresponding author. Tel. +33-144-275562; fax: +33-144-273841.
E-mail address: miv@ccr.jussieu.fr (M. Verdaguer)

PII: S0010-8545(99)00156-3

Abstract

This paper was presented as a session lecture at the XXXIII ICCC in Florence (29 August–4 September 1998). It intends to point out some recent achievements in the chemistry and physics of transition metal polycyanides in the field of molecular magnetism. Prussian blue is sometimes considered as the first coordination compound and the paper shows how it is possible to obtain brand new results with Prussian blue analogues when looking at these antique systems with fresh eyes. Hexacyanometalates revealed in the last few years as very flexible molecular precursors to build three-dimensional molecule-based magnets with tunable and high Curie temperatures or to grow high nuclearity clusters with tunable high spins and anisotropy. The use of a localized electron orbital model allowed the authors' team to push the Curie temperatures from 5.6 K in the Prussian blue itself to above room temperature in a vanadium–chromium Prussian blue analogue. Several groups confirmed the result and are improving it. In the same way, high spin molecules with ground spin states ranging from $S = 3/2$ to $27/2$ were obtained. The paper reviews some of the steps which lead to these spectacular findings and some of the prospects opened in molecular materials by this revival of polycyanide chemistry.

Keywords: Theoretical methods: orbital model of exchange interaction; Phenomena: molecular magnetism, photomagnetism; Materials: Prussian blues, high spin molecules; Applications: magnetic devices

1. Introduction

The story began in 1704. At this time a Berliner draper, M. Diesbach prepared for the first time, in a strange way, a bright blue pigment. He boiled beef blood in a strongly basic medium and he was surprised to get a blue coloration [1]. At this time, neither cyanide nor hexacyanometalates were known but Prussian blue was born, which is sometimes recognized as the first coordination compound.

Nowadays, it is much more convenient to prepare Prussian blue from aqueous solutions of hexacyanoferrate(II) and iron(III) chloride. A lecture demonstration consists in placing on one side of a petri dish a few crystals of potassium hexacyanoferrate(II) and at the opposite a few crystals of iron(III) chloride. Water is then carefully poured in between so that the crystals are slowly dipped in water. After a while, a beautiful blue colour develops at the interface where the convexion movement brings together the dissolved reactants. This experiment can be easily exploited to demonstrate that (i) Prussian blue and its derivatives can be used as industrial pigments; (ii) mild chemistry, at room temperature (r.t.) and pressure, in aqueous solution, can be used to build solids from molecules.

Indeed, the formula of the genuine Prussian blue is $Fe(III)_4[Fe(II)(CN)_6]_3 \cdot 14H_2O$ [2]. The structure was first proposed by Keggin and Miles [3] and then reformulated by Ludi and Güdel [4]. Prussian blues build a large family of cubic systems

$C_nA_p[B(CN)_6]_q \cdot xH_2O$ where A occupies all the summits and all the centres of the faces and the $[B(CN)_6]$ are located at the octahedral sites. C is a monovalent cation which can be inserted in part of the tetrahedral sites of the cubic structure. The reaction leading to the neutral solid is a simple Lewis acid–base interaction:

$$q[B(CN)_6]^{p-}_{aq} \text{ (Lewis base)} + pA^{q+}_{aq} \text{ (Lewis acid)} \rightarrow \{A_p[B(CN)_6]_q\}^0 \cdot xH_2O \text{ (s)}$$

The bonding molecular orbitals implied in the acid–base interaction do not concern the unpaired electrons, which remain in non bonding or antibonding orbitals and give rise to various magnetic properties.

Three kinds of structures appear in Fig. 1. The two first present an A/B 1:1 stoichiometry; in this case, the coordination spheres of A and B are $\{A(NC)_6\}$ and $\{B(CN)_6\}$; A(B) has six B(A) neighbours; the third structure displays a A/B 3:2 stoichiometry, with one third of $[B(III)(CN)_6]$ vacancies filled by water molecules; the B coordination sphere is left unchanged but the mean coordination sphere of A becomes $\{A(NC)_4(H_2O)_2\}$. The mean number of B neighbours around A is now four.

This simple and appealing structure is reminiscent of the well-known perovskites. Nevertheless, our X-ray spectroscopy experience (EXAFS at the K edges of the transition metals) demonstrates that the molecular precursor, $[B(CN)_6]$, remains practically an unchanged building block in the solid state. The Prussian blue analogues usually present a cell parameter ranging from 10.0 to 10.9 Å [4]. This value corresponds to the A–A (B–B) distances between two identical metallic ions in the network. In the Prussian blue itself, the Fe(III) cations are divided by 10.18 Å, separated by the $[Fe(II)(CN)_6]^{4-}$ entities [2], that explains that the material behaves magnetically has a paramagnet with very weak interactions between two neighbouring magnetic centres which are high spin d^5 Fe(III) ($S = 5/2$). As for the d^6 Fe(II) centres, they are low spin and diamagnetic. The –{NC–Fe(II)–CN}–

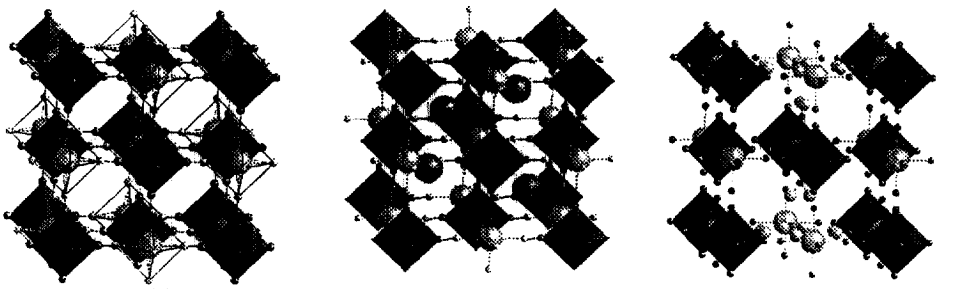

Fig. 1. Typical structures of cubic Prussian blue: (a) $A(III)[B(III)(CN)_6]$, A_1B_1; (b) $Cs(I)A(II)[B(III)(CN)_6]$, $Cs_1A_1B_1$; (c) $\{A(II)\}_3[B(III)(CN)_6]_2 \cdot xH_2O$, A_3B_2. $[B(CN)_6]$ are the dark solid octahedra surrounded by CN (very small spheres), A are the light small spheres, C are the grey medium size spheres in (b); in (c) H_2O are shown by the small light-grey spheres.

bridge between two Fe(III) provides nevertheless some electron delocalization pathway, as studied by Day and Robin [5], and a magnetic order appears below 5.6 K [6].

We looked at this old system with new eyes some time ago [7,8] and it appeared to us that: (i) the use of hexacyanometalates as starting building blocks could open the possibility to develop orbital interactions in the three directions of space. At this time most of the research teams were engaged in the study of low dimensional systems and therefore the observed Curie temperatures were remaining very low [9]. The first r.t. V-TCNE magnet remained a superb exception [10]; (ii) the Prussian blue matrix can accommodate, at will—at least in principle—very different A and B paramagnetic ions and therefore offers a large flexibility for the design of a wide range of materials; (iii) the high symmetry of the system, with the linear A–NC–B alignment, allows an efficient control of the nature and of the amplitude of the exchange interaction between A and B; (iv) a new and versatile playground therefore becomes available to produce new magnetic objects. We gave the general recipes in references [11–15]; the details for three-dimensional systems can be found in references [16–22] and in references [23–27] for lower dimensionality types.

The field was not completely unexplored since pioneers like Anderson and Bozorth in the 1950s [28,29], Klenze [30] and Babel in the 1980s [31,32] published important data. The first attempts [28] were not performed with samples chemically pure enough to reach safe conclusions. Instead, Babel brought a lot of new important information [31,32]. In an extensive study of bimetallic Prussian blue analogues with only one magnetic ion among A and B, he demonstrated that Curie laws were obtained. When the two metallic centres A and B are both paramagnetic, strong interactions can be achieved: with Cs(I)Mn(II)[Cr(III)$(CN)_6$] Babel was able to reach a Curie temperature above liquid nitrogen, $T_C = 90$ K [31].

Chemists engaged in molecular magnetism are accustomed to claims about the versatility of coordination and molecular chemistry to vary at will the final properties of their systems. Nevertheless, except for the V-TCNE system described by Miller [10], in the beginning of the 1990s no molecule-based magnet presented a Curie temperature close or above r.t. The first challenge was therefore clear: to reach a three-dimensional magnetic ordering temperature above r.t. in a Prussian blue system, to demonstrate the feasibility of the molecular approach to get high T_C systems, to obtain r.t. magnets and to use them in devices. In such cases, two ways are open: (i) serendipity (after a systematic study of all A/B transition pairs used to build Prussian blues), it can be a long way; (ii) a more rational approach based on what we know on the interaction between two paramagnetic ions through a molecular bridge. We chose the second approach and we made use of two models, apparently far apart: the molecular field approach, as used by Néel in three-dimensional systems and well known among physicists and solid state chemists [33–35], and the orbital model of exchange interaction designed by Hoffmann [36] and Kahn [37,38] to deal with binuclear or low-dimensional systems.

2. Models to foresee Curie temperatures and the nature of the exchange interaction

The expression given by Néel in his 1948 paper [33] to fit the susceptibility of ferrimagnets in a range of temperature close to the ordering temperature, allows one to extract the following very useful relation:

$$kT_C = \{z|J|\sqrt{(C_A C_B)}\}/(N_A g^2 \beta^2) \quad (1)$$

z is the number of magnetic neighbours, $|J|$ is the absolute value of the exchange interaction, C_A and C_B are the Curie constants of A and B, N_A is the Avogadro constant, g is a mean g (Lande) factor and β is the Bohr magneton. Everything being equal, to increase T_C, it is therefore possible to play (i) on the stoichiometry (to enhance z) and (ii) on the nature and the amplitude of the interaction (to enhance $|J|$). The higher z and $|J|$ are, the higher the T_C is.

z is fixed and controlled by the stoichiometry; its maximum is six with hexacyanometalates in an A/B 1:1 system. It becomes four in the most frequently encountered A/B 3:2 systems. The less the vacancies are, the higher the T_C is.

To foresee the $|J|$ value, the Hoffmann (orthogonalized magnetic orbitals) or Kahn (non orthogonalized magnetic orbitals) orbital models can be made use. Both models predict that: (i) orthogonal orbitals give rise to ferromagnetism; (ii) overlapping orbitals give rise to antiferromagnetism.

Two expressions summarize the models in the case of two electrons 1 and 2 on two sites, described by two identical orbitals a and b. The singlet–triplet energy gap $J(J = E_S - E_T)$ is given by:

$J = 2k + 4\beta S$ (a) Kahn's model [37]

$J = 2K_{ab} - (e_1 - e_2)^2/(J_{aa} - J_{ab})$ (b) Hoffmann's model [36]

(2a,b)

In (a): k is the bielectronic exchange integral (positive) between the two non orthogonalized magnetic orbitals a and b; β is the corresponding monoelectronic resonance or transfer integral (negative) and S the monoelectronic overlap integral (positive) between a and b; in (b): K_{ab} is the bielectronic exchange integral (positive) between two identical orthogonalized magnetic orbitals a′ and b′; $(e_1 - e_2)$ is the energy gap between the molecular orbitals Ψ_1 and Ψ_2 built from a′ and b′, J_{aa} is the bielectronic interelectronic repulsion on one centre and J_{ab} the equivalent on two centres. Both J expressions contain a positive term, J_F, favouring a parallel alignment of the spins and ferromagnetism, and a negative term, J_{AF}, favouring an antiparallel alignment of the spins and short range antiferromagnetism. The total interaction results from the addition of the two terms $(J = J_F + J_{AF})$. When the two a and b orbitals are different no rigorous analytical treatment is still available; a semi-empirical relation was proposed by Kahn [38]:

$$J = 2k + 2S(\Delta^2 - \delta^2)^{1/2} \quad (3)$$

where δ is the initial energy gap between a and b orbitals, Δ is the energy gap between the molecular orbitals built from them.

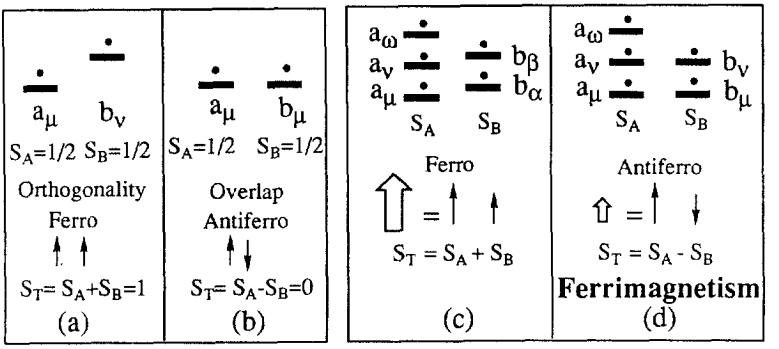

Fig. 2. Spin coupling between two identical spins: (a) ferromagnetism; (b) antiferromagnetism; spin coupling between different spins: (c) ferromagnetism; (d) ferrimagnetism.

When several electrons are present on each centre, n_A on one side, n_B on the other, J can be described as the sum of the different 'orbital pathways' $J_{\mu\nu}$, weighted by the number of electrons [38,40] (μ and ν are symmetry labels):

$$J = (\sum_{\mu\nu} J_{\mu\nu})/n_A\, n_B \tag{4}$$

When only one electron is present per site, the situation is simple: short range ferromagnetic interaction leads to the triplet; short range antiferromagnetic interaction leads to the singlet. When each site bears a different number of electrons, the short range ferromagnetic coupling leads to a total spin ground state which is the sum of the spins: $S_T = S_A + S_B$; the short range antiferromagnetic coupling leads to a total spin ground state which is the difference of the spins: $S_T = |S_A - S_B|$. Fig. 2 illustrates these conclusions. One of the key points is that antiferromagnetism between two neighbours bearing different spins leads to a magnetic ground spin state. After Néel [33], this situation is known as ferrimagnetism. In this case, the value of the ground spin state is smaller than it would be for the ferromagnetic coupling. Nevertheless, overlap and antiferromagnetism can be used to get magnetic situations. In other words, ferrimagnetism is a friendly process which transforms a phenomenon (antiferromagnetism) in its contrary (magnetism).

3. Application of the models to the Prussian blues

3.1. Orbital analysis in a binuclear $(CN)_5$–A–NC–B$(CN)_5$ unit

The qualitative application of such models to the Prussian blues is a case study which can be used as a textbook example. Indeed, at the B site, the paramagnetic ion B is always surrounded by six cyanides bonded through carbon atoms [$B(CN)_6$], i.e. a high field low spin site. We are aware of course of the possibility of the cyanides to flipping, and to create B–NC bonds during the synthesis, but we shall

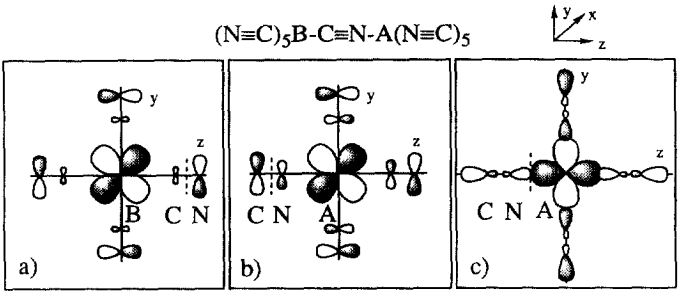

Fig. 3. Local magnetic orbitals in an isolated $(NC)_5$–B–CN–$A(NC)_5$ binuclear unit: (a) t_{2g} magnetic orbitals at the B site; (b) t_{2g} magnetic orbitals at the A site; (c) e_g magnetic orbitals at the A site.

avoid these situations. Only the t_{2g} orbitals are occupied (there is no known d^n B ion with $n > 6$ in $[B(CN)_6]$ complexes). At the A site, in a A_1B_1 stoichiometry, the A ion is surrounded by six nitrogen atoms $[A(NC)_6]$; in a A_3B_2 stoichiometry, the A coordination sphere is a mixture of nitrogen (from cyanides) and oxygen atoms (from coordinated water molecules): $[A(NC)_{6-x}(OH_2)_x]$ $(x = 0–6)$. In both cases, the site is mean or low ligand field and therefore A is expected to be high spin. Nevertheless, in border line cases (Cr(II), Mn(III), Co(II), see below), it is not impossible to expect and to observe a low spin behaviour. The singly occupied orbitals (or magnetic orbitals) on both side are sketched in Fig. 3: (a) t_{2g} magnetic orbitals at the B site; (b) t_{2g} magnetic orbitals at the A site; (c) e_g magnetic orbitals at the A site. The dotted lines schematize the nodal surface of the orbitals on the internuclear axis. Magnetic orbitals are either non bonding or antibonding; the unpaired electrons do not participate to the stability of the bond.

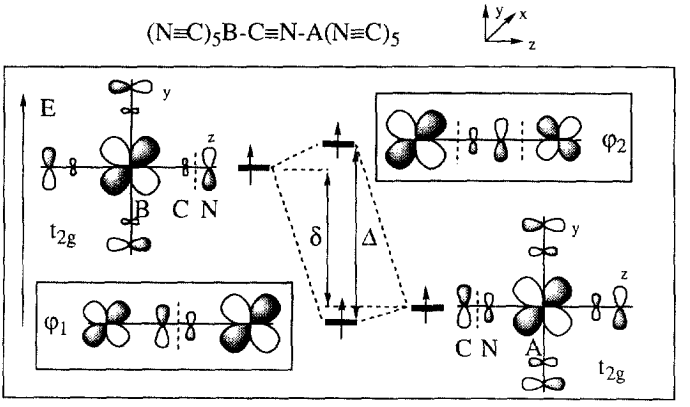

Fig. 4. Molecular orbitals φ_1 and φ_2 built from t_{2g} orbitals in the $(NC)_5$–B–CN–$A(NC)_5$ binuclear unit.

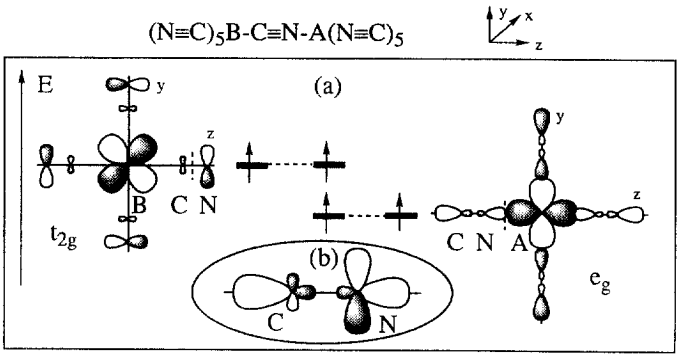

Fig. 5. Orthogonal magnetic orbitals in the $(NC)_5$–B–CN–A$(NC)_5$ binuclear unit: (a) orthogonal $t_{2g}(B)$ and $e_g(A)$ orbitals left unchanged in the binuclear unit; (b) insert: spin density in two orthogonal p orbitals of nitrogen (p_y and p_z).

The molecular orbitals (MO) built from the linear combination of the t_{2g} orbitals appear in Fig. 4:

bonding MO: $$\varphi_1 = \lambda_+ \; t_{2g}(B) + \mu_+ \; t_{2g}(A) \qquad (\lambda_+ \ll \mu_+) \tag{5a}$$

antibonding MO: $$\varphi_2 = \lambda_- \; t_{2g}(B) - \mu_- \; t_{2g}(A) \qquad (\lambda_- \gg \mu_-) \tag{5b}$$

The weight of the two metals is different in the two MOs. Our representation enhances the A–B mixing, which is much smaller than the one shown.

The energy between the magnetic orbitals is initially δ; after interaction the energy gap between φ_2 and φ_1 is Δ. The dotted lines display the nodal surfaces in the orbitals along the internuclear axis: one in the bonding, two in the antibonding one.

The interaction between orthogonal $t_{2g}(B)$ and $e_g(A)$ orbitals is shown in Fig. 5(a). In the insert (Fig. 5(b)), we emphasize the spin density borne by the nitrogen in the two orthogonal p_y and p_z orbitals. The overlap density

$$\rho = t_{2g}(B)\; e_g(A) \tag{6}$$

is strong on the nitrogen and from this situation, we expect a strong ferromagnetism interaction since the exchange integral $k \propto \rho^2$ [39]. In all the cases, Figs. 4 and 5 display the triplet configuration.

The conclusions from Figs. 4 and 5 are simply drawn: (1) the $t_{2g}(B)$–$e_g(A)$ pathways lead to ferromagnetic F interactions, expected to be important, thanks to the electronic structure of the cyanide bridge and the special role of nitrogen; (2) the $t_{2g}(B)$–$t_{2g}(A)$ pathways lead to antiferromagnetic AF interactions; the larger the $(\Delta - \delta)$ gap, the larger $|J|$.

We can use this orbital analysis to foresee the nature of the interaction of various A paramagnetic cations with $[Cr(III)(CN)_6]$, chosen because Cr(III) is d^3 ($(t_{2g})^3$, $S = 3/2$) and provides spin density in the three directions of space. The number and the nature of the exchange pathways are schematized in Fig. 6 and summarized in

Table 1 for known divalent cations A(II) of the first period of the transition elements, from Ti(II) to Cu(II).

3.2. Testing the model in selected Prussian blue analogues

A first test of the validity of the model is to check that a compound where only ferromagnetic pathways are foreseen, Cs(I)Ni(II)[Cr(III)(CN)$_6$]·2H$_2$O, is really ferromagnetic. We found a ferromagnetic long range order at $T_C = 90$ K, the same temperature as in Babel's Cs(I)Mn(II)[Cr(III)(CN)$_6$] system. The T_C value is non negligible, supporting the conclusions of Fig. 5 concerning the strength of ferromagnetic pathways. It is even possible to compare the J values in the Ni and Mn derivatives from formulae (1) and (4), to find that $J_{CrNi} \approx 2J_{CrMn}$ and that J_F, the mean value of the ferromagnetic orbital pathways and J_{AF}, the antiferromagnetic one, are roughly equal in absolute value.

A second test is to check the Néel prevision ($T_C \propto z$). For that, it is possible to compare the Curie temperatures of two A_2B_3 systems with $z_1 = 4$ magnetic neighbours {Ni(II)}$_2$[Cr(III)(CN)$_6$]$_3$ ($T_C = 53$ K) and {Mn(II)}$_2$[Cr(III)(CN)$_6$]$_3$ ($T_C = 60$ K) with the corresponding A_1B_1 ($T_C = 90$ K), $z_2 = 6$ magnetic neighbours. The prevision works rather well (Table 1): the ratio between the T_Cs is 1.8/3 in the Ni(II) system and 2/3 in the Mn(II) system, close to the expected $z_1/z_2 = 2/3$. Later on, we checked the validity of the orbital model on cluster systems with dimension zero where it is possible to find directly the J values from susceptibility measurements (see below).

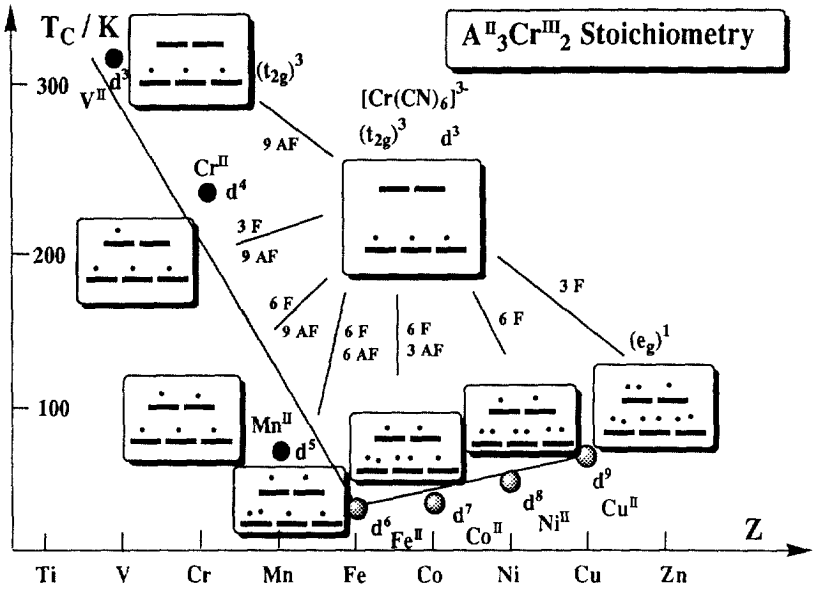

Fig. 6. Experimental variation of T_C with Z, the atomic number of the A(II) cation in the series {A(II)}$_3$[Cr(III)(CN)$_6$]$_2$, electronic structures and expected exchange pathways (black dots, ferrimagnets, grey dots ferromagnets).

Table 1
Electronic structure, exchange pathways and interactions in A(II)–NC–Cr(III) magnetic pairs

Cr(III) $(t_{2g})^3$	Ti(II) $(t_{2g})^2$	V(II) $(t_{2g})^3$	Cr(II) $(t2g)^3(eg)^1$	Mn(II) $(t2g)^3(eg)^2$	Fe(II) $(t2g)^4(eg)^2$	Co(II) $(t2g)^5(eg)^2$	Ni(II) $(t2g)^6(eg)^2$	Cu(II) $(t2g)^6(eg)^3$
AF pathways	6	9	9	9	6	3	0	0
F pathways	0	0	3	6	6	6	6	3
Interaction[a]	AF	**AF**	**AF**	**AF**	*af*	*af*	**F**	**F**
T_C/K		**315**	**240**	**60**	*16*	*23*	**53**	**66**

[a] Nature of the interaction foreseen in the hypothesis where the antiferromagnetic interactions are larger that the ferromagnetic ones. F, ferro; AF, antiferro; af, weak antiferromagnetic interaction. In bold, the cases when the prediction of the model holds when compared to the experimental results in a series of $A(II)_3[Cr(III)]_2$ derivatives, in italic the ones when the model fails. No Ti(II) derivative is known up to now.

3.3. How to reach room temperature?

The second step is to apply the model to enhance the Curie temperature. It is important to remember at this point that the ferromagnetic exchange pathways are non negligible: in a ferrimagnetic system if one wants to enhance the absolute value of $|J|$, it is necessary to decrease the ferromagnetic contribution. Table 1 clearly shows that the goal can be achieved when going from Mn(II) to V(II) through Cr(II). Fig. 6 illustrates the observed changes in T_C versus Z, the atomic number in the series $\{A(II)\}_3[Cr(III)(CN)_6]_2$ and compares it with the nature of the exchange pathways.

Indeed the model works pretty well [41]. Starting from 60 K in the Mn(II) derivative, we found 240 K in the Cr(II) derivative [18] and 315 K in V(II) [19]. It is important to point out that in $\{V(II)\}_2[Cr(III)(CN)_6]_3$, the spin on the vanadium(II) is the same as the one on chromium(III), $S = 3/2$. A $V(II)_1Cr(III)_1$ would be strictly antiferromagnetic with an exact compensation of the spins. Instead, with a $V(II)_3Cr(III)_2$ stoichiometry ferrimagnetism arises from the non compensation of the spins. It can be seen in Fig. 6 that the model fails in the cases of the iron and the cobalt derivatives: the exchange is ferromagnetic instead of the expected antiferromagnetic. As ever, reality is more complex than any model. In the case of weak interactions (and weak T_C), the localised electron model appears insufficient: if some electron delocalisation takes place, a double exchange mechanism is able to favour a ferromagnetic coupling [42]. Other teams are working successfully along the same reasoning as ourselves on different systems [43–49]. Even when the model gives good prevision, reality is always more complex: the $\{Cr(II)\}_3[Cr(III)(CN)_6]_2$ system is made of Cr(II), but there is a mixture of low spin and high spin [18]. Two teams were able to improve the T_C and other properties by playing on the non stoichiometry of the system [48,49]. The expected $\{V(II)\}_3[Cr(III)(CN)_6]_2$ is in fact an amorphous, non stoichiometric compound, deep blue mixture of V(II) and V(III): $\{V(II)\}_x\{V(III)\}_{(1-x)}[Cr(III)(CN)_6]_{0.86}\cdot 2.8H_2O$, with $x = 0.42$. The compound is very sensitive to dioxygen [19]. The magnetization at saturation is very weak ($0.15\mu_B$) and fits perfectly with the proposed formulation. The coercive field is the one of a very soft magnet (25 Oe at 10 K). Even if the system is considered as a cornerstone in the saga of molecular magnetism [41], it is far from being perfect.

3.4. Improving the magnetic properties of room temperature molecule-based magnets

In order to change and to try to improve the properties of the samples, to obtain better characterized materials, polycrystalline ones, etc. the usual way for the chemist is to vary the synthetic conditions. We undertook new syntheses of the room T_C bimetallic chromium–vanadium and we obtained a set of non stoichiometric Prussian blue analogues $C(I)_yV[Cr(III)(CN)_6]_z\cdot nH_2O$ (C, alkali cation) with T_C varying between 295 and 330 K. We are not alone in such attempts and Girolami, Miller, Hashimoto and others are working in the same field [47]. When

looking at the structure (Fig. 1(c)), one realizes how the structure of Prussian blue is rich in vacancies and channels which can accommodate guest molecules (anions, cations, solvent), which can either improve or compromise the structural organisation of the material. Indeed, many factors play an important role not only in the successful synthesis of the compounds in the VCr series but also in the magnetic properties (Curie temperature, magnetisation at saturation, coercivity). Among them are the structure and the stoichiometry (presence of counterions, solvent), the oxidation state and the electronic structure of the vanadium ions, the cristallinity and the size of the particles. In a long term endeavour to master these parameters, we studied the influence of four factors: the influence of aerobic conditions, the addition of cationic species, the nature of the counteranion (size, coordination ability) and the nature of the solvent [51].

Prepared in aerobic conditions, the vanadium/chromium system gives a crystalline dark green $\{VO(IV)\}_3[Cr(III)(CN)_6]_2$ with a much lower Curie temperature (115 K) [21,50]. Fig. 7 shows the thermal variation of the magnetization in the V(II) and in the VO(IV) systems. The minimum in the $\chi_M T$ curve versus T is a clear signature of ferrimagnetism. The result shows that anaerobic conditions are necessary to maintain high T_Cs.

Then, we varied the stoichiometry by the addition of cationic species in the tetrahedral holes of the Prussian blue structure [23]. From the molecular precursor $[Cr(III)(CN)_6]^{3-}$ and from vanadium V(II) salts, we got two new bimetallic chromium–vanadium ferrimagnets, either **1** (in absence of Cs(I): $\{V(II)_{0.45}V(III)_{0.53}(V(IV)O)_{0.02}[Cr(CN)_6]_{0.69}(SO_4^{2-})_{0.23}(K_2SO_4)_{0.02}\}\cdot 3H_2O$ or **2** (in presence of Cs(I)): $\{Cs(I)_{0.82}V(II)_{0.66}(V(IV)O)_{0.34}[Cr(CN)_6]_{0.92}(SO_4^{2-})_{0.20}\}\cdot 3.6H_2O$. The two systems present a larger magnetisation than the first reported V–Cr analogue (0.36 $N_A\beta$ for **1** and 0.40 $N_A\beta$ for **2**). The antiparallel alignment of the neighboring spins in the magnetically ordered phase leads to a resulting total magnetization M_T which is the difference between the magnetisation arising from the subset of chromium ions M_{Cr} and the one from the subset of vanadium ions, M_V:

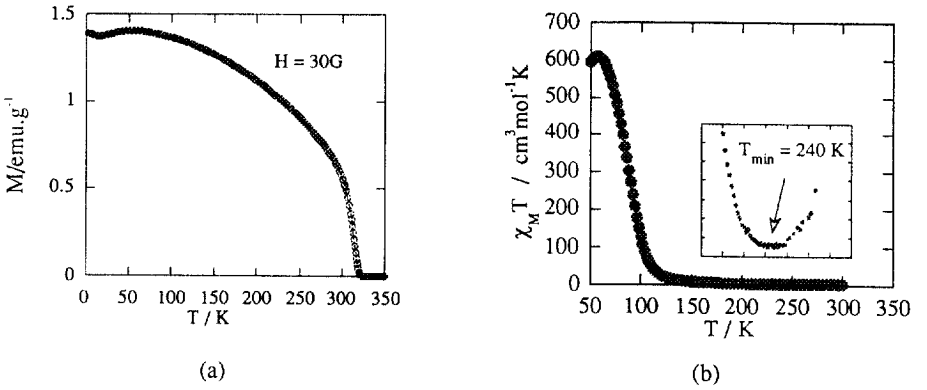

Fig. 7. Thermal variation of (a) the magnetisation in $V(II)_{0.42}V(III)_{0.58}[Cr(III)(CN)_6]_{0.86}\cdot 2.8H_2O$; (b) the $\chi_M T$ product in $\{VO(IV)\}[Cr(III)(CN)_6]_{2/3}\cdot 10/3H_2O$.

$$M_T = |M_{Cr} - M_V| \tag{7}$$

Two situations may arise, one when the larger magnetic moments are borne by the chromium ions and are aligned parallel to an external applied field ($M_{Cr} > M_V$); the other when $M_V > M_{Cr}$. In the later case, the sign of the quantity ($M_{Cr} - M_V$) is reversed and the magnetic moments of vanadium ions now lie parallel to the field.

For example, for analogues of compound **1** $(C(I)_yV(II)_\alpha V(III)_{1-\alpha}[Cr(III)(CN)_6]_z \cdot nH_2O$, it is shown in [22] that

$$M_T = -(3z - \alpha - 2) \tag{8}$$

The spin values of these compounds can be represented in a three-dimensional space, versus α, varying between 0 and 1, and versus z, varying between 2/3 and 1. The spin values are described by plans presented in Fig. 8 for the analogues of **1**.

The calculated M_T value is positive for **1** ($M_T = +0.36N_A\beta$) and negative for **2** ($M_T = -0.42N_A\beta$). The absolute values are in good agreement with the experimental ones. The crucial difference between the two compounds is the sign of M_T, influenced by the balance between the values of z (Cr(III)/V ratio) and α the V(II)/V ratio. Conventional magnetization measurements give the absolute value of the macroscopic magnetization but not the local magnetization. Instead, X-ray magnetic circular dichroism (XMCD), a new X-ray spectroscopy developed with synchrotron radiation, is an element and orbital selective magnetic local probe. Direct information is obtained about the local magnetic properties of the photon absorber (direction and magnitude of the local magnetic moment). The signal appears whatever the shape of the sample (crystals, powders etc.). The spin-polarized neutron diffraction gives analogous results but requires long range structural order and large single crystals. XMCD is better adapted for poorly organized materials.

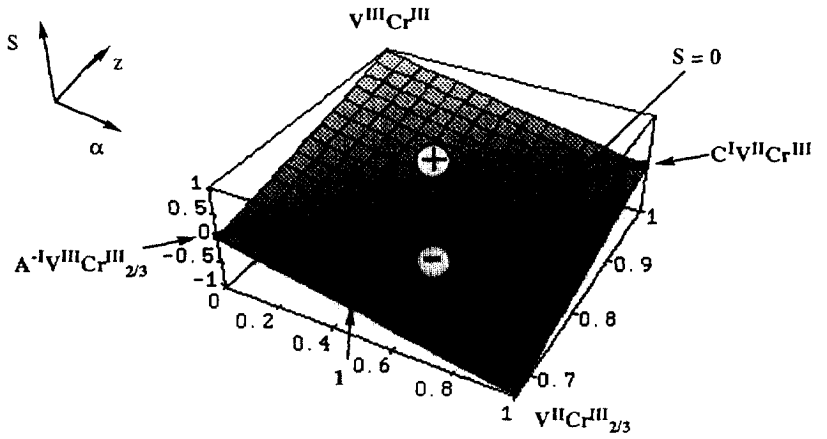

Fig. 8. Variation of the spin values S versus z and α parameters for compounds $C(I)_yV(II)_\alpha V(III)_{1-\alpha}[Cr(III)(CN)_6]_z \cdot nH_2O$. **1** is in the part of the plane where the total spin has the same direction as the vanadium spins.

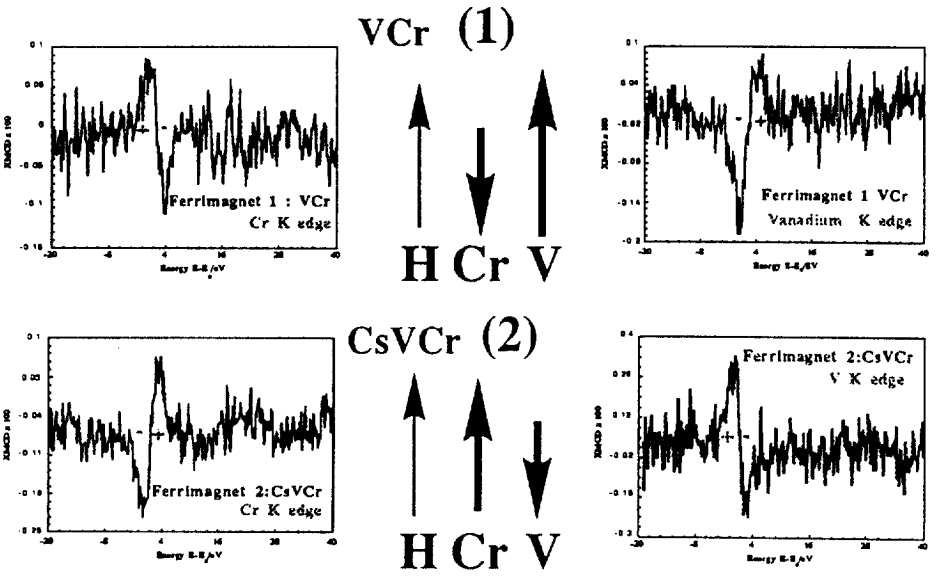

Fig. 9. Dichroïc signals at the V and Cr K edges for compounds **1** and **2**.

The results of our XMCD experiments at the K edges of vanadium and chromium are reported in Fig. 9. They show:

-the antiferromagnetic coupling between vanadium and chromium ions (inversion of the dichroic signal at the vanadium and the chromium K edges, for each compound);

-the ability of the vanadium–chromium ferrimagnets to change the bearer of the majority spin, through the modification of the chemical composition (for a given edge, the general shape of the dichroïc signal of **1** is the opposite of the one found in **2**);

-the usefulness and the validity of XMCD to determine locally the spin orientation on each metal ion in this kind of materials.

The absolute orientation of the magnetic moments proposed in Fig. 9 results from a complementary XMCD experiment on the ferromagnetic $CsNi[Cr(CN)_6]$ where all the magnetic moments are aligned parallel to the applied field with a dichroïc signal for chromium similar to that of **2**.

Further useful applications of X-ray absorption (EXAFS, XANES at the K and $L_{2,3}$ edges and XMCD) in the study of Prussian blues can be found in references [52–54].

Finally, we studied the influence of two other parameters: nature of counterions and solvents. The reaction of $[Cr(CN)_6]^{3-}$ in H_2O (as solvent) with the Tutton salt $K_2V(II)(SO_4)_2{\cdot}6H_2O$ as the starting material and SO_4^{2-} as counteranion, gives compound **3**: $\{V(II)_{0.78}V(III)_{0.22}[Cr(CN)_6]_{0.56}(SO_4^{2-})_{0.28}(K^+)_{0.11}\}{\cdot}4H_2O$. Instead, the reaction carried out in H_2O with $[V(MeOH)_6]I_2$ as the starting material and I^- as counteranion gives compound **4**: $\{V(II)_{0.58}V(III)_{0.42}[Cr(CN)_6]_{0.77}(I^-)_{0.2}(NBu_4^+)_{0.1}\}$

·$5H_2O$. Finally, when the reaction is performed in methanol as the solvent and $[V(MhOH)_6]I_2$ as the starting material, compound **5** is obtained: $\{V[Cr(CN)_6]_{0.69}(I^-)_{0.03}\}\cdot 1.5MeOH$. The magnetisation versus temperature curves of the different compounds are shown in Fig. 10. The Curie temperatures are different (295 K for **3**, 330 K for **4** and 200 K for **5**) as well as the magnetisation at saturation ($M/N_A\beta = 1\mu_B$ for **3**, 0.26 μ_B for **4** and evanescent for **5**).

It can be concluded that the counteranions and the solvents have large effects on the Curie temperatures and on the magnetisation at saturation as well. The large size and weak coordinating anions, like I^- do not induce disorder in the structure and the magnetic properties are improved. As for the solvent, its influence is more complex. The main influence appears to be in the number of magnetic neighbours (which is proportional to T_C after Néel's equation (1)). In $[V(solvent)_6]^{2+}$, when the kinetics of solvent exchange is faster (with water, compared to methanol or to other organic solvents), the substitution of the solvent molecules by CN^- around V^{2+} is more effective and the number of interactions between Cr and V increases [51].

4. New achievements and prospects

When the main features of a given system (here the magnetic Prussian blues) are understood, time comes to explore other directions. The Prussian blue structure offers such a versatile matrix and polycyanides are such versatile precursors that beyond the high T_Cs systems quoted above, complete new and exciting topics can be attacked.

We are now exploring new systems with other precursors, bearing more diffuse magnetic orbitals. Our first attempts with $[W(CN)_8]^{3-}$ are reported in [51].

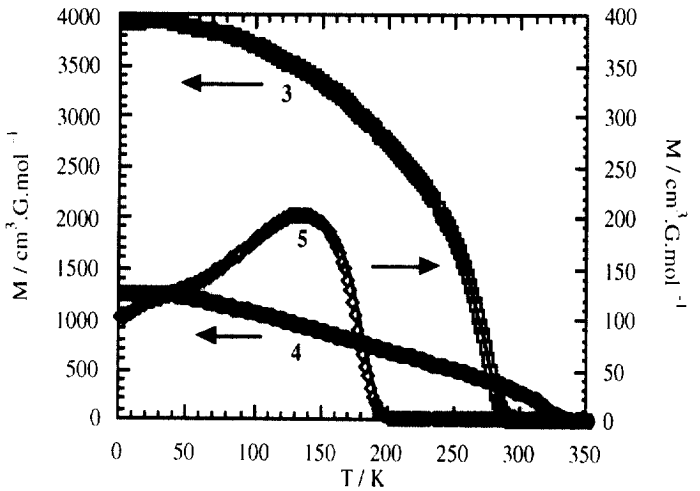

Fig. 10. Thermal variation of the magnetization of the three vanadium–chromium compounds **3**, **4** and **5**.

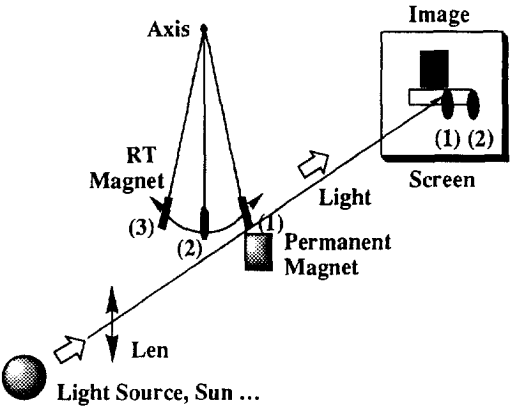

Fig. 11. Scheme of a device using the properties of a r.t. magnet to transform light in mechanical energy.

We give hereunder some directions that we are exploring: magnetic devices, magneto-optical properties (how molecule-based magnets can modify light), photomagnetism (how light can dramatically affect magnetic properties of molecule-based magnets etc.).

4.1. Devices from room temperature magnets

Once r.t. is reached, it becomes possible to think about applications and design of devices. A molecule-based magnet such as our vanadium–chromium system ($T_C = 42$°C), can be a useful tool to illustrate easily, near r.t., what is a Curie temperature. Fig. 11 displays a demonstrator designed for this purpose.

The compound is sealed in a glass vessel under argon and suspended at the bottom of a pendulum (equilibrium position (2) in absence of permanent magnet). It is then cycled between its two magnetic states: the 3D-ordered ferrimagnetic one, when $T < 42$°C and the paramagnetic one, when $T > 42$°C. The three steps are: (1) the r.t. magnet is cold ($T < T_C$, ferrimagnetic state). It is attracted ($\rightarrow$) by the permanent magnet and deviates from the vertical direction. Its temperature increases since it is heated by a light beam focused at position (1) above the permanent magnet; (2) the r.t. magnet is hot ($T > T_C$ paramagnetic state). It is no longer attracted and is moving away from the magnet ($\leftarrow$), under the influence of its own weight. Its temperature decreases since it is air-cooled; (3) the r.t. magnet is now cold ($T < T_C$). It is again attracted by the permanent magnet ($\rightarrow$) and will come back to position (1) where the process is ready for a new oscillation. The frequency of the oscillating movement depends on various parameters: magnetic energy of the permanent magnet, weight of the sample, heating power of the light source and r.t. The demonstrator, beating the second, is operating for a long time in our laboratory and millions of cycles have been accomplished without any fatigue. The device is an example of a thermodynamical machine working between two energy reservoirs with close temperatures (light and shadow) allowing the

conversion of light into mechanical energy. We are now exploring other practical applications: thermal probes, magnetic switches, and so on.

4.2. Thin layers

Magnetic Prussian blue analogues display bright colours and transparency, among other interesting properties. To exploit this capability, it is useful to prepare thin films (a vanadium–chromium 1 μm thick film is indeed quite transparent). The best way to prepare such films is electrochemical synthesis. Various thin films have been prepared from transition metal hexacyanoferrates in the recent years on various substrates and under different operating conditions [55]. To obtain thin films of r.t. molecule-based magnets, one must deeply modify the experimental conditions since one actually wants to produce and to stabilise highly oxidisable ions such as Cr(II) [56] or V(II) [57]. Thus, strongly negative potentials must be applied at the working electrode. Moreover, to avoid the oxidation of the sample, which would lead to the dramatic drop in the Curie temperature as quoted above [50], the atmosphere and the solutions must be oxygen-free during both the preparation and the characterisation of the sample. The magnetisation of a transparent magnetic film can then be probed by measuring the Faraday effect in the sample. The Faraday effect corresponds to spin-dependent modifications of the polarisation of the transmitted light. It can be related to the circular magnetic dichroism. Spectroscopic measurements in the UV–vis range bring information about the magnetisation of the sample and moreover about its electronic structure. Besides, observing the Faraday effect at r.t. in these compounds is the first step to demonstrating the capability of these materials to be used as media in magneto-optical data storage. We have succeeded in obtaining for the first time in a r.t. magnet (a vanadium–chromium derivative) a magneto-optical signal at r.t. and further studies are underway in this promising area [57].

4.3. Photomagnetism

A new area opened 2 years ago, when Hashimoto and his team reported in a Prussian blue analogue close to $Co(II)_3[Fe(III)(CN)_6]_2 \cdot nH_2O$ or Co_3Fe_2, a well known system, the existence of an exciting photomagnetic effect [58]. The Curie temperature of the initial system is low ($T_C \approx 15$ K) but the physics of the phenomenon deserves interest, since a photoexcitation at the molecular level gives rise to a modification of the macroscopic properties of the material [59]. Starting from aqueous solutions of Co(II) and hexacyanoferrate(III), Hashimoto obtained a powder which exhibited a photo-induced enhancement of the magnetisation at low temperature and an increase of the Curie temperature [58]. The explanation proposed was related (i) to the presence of isolated diamagnetic pairs Co(III)–Fe(II) in the compound, otherwise built from –Co(II)–NC–Fe(III)– units and (ii) to a photo-induced electron transfer from Fe(II) to Co(III) through the cyanide bridge. The enhancement of the magnetisation and the increase of the Curie temperature

simply follows from the increase of the number of magnetic pairs in the material (Eq. (1)). The key of the phenomenon would then be the presence of diamagnetic pairs in the framework [60–66].

The synthesis of the Prussian blue analogues involves the substitution of water molecules of $[Co(II)(H_2O)_6]$ by $[Fe(III)(CN)_6]$. This means a progressive increase of the cobalt ligand field, when oxygen atoms are replaced by nitrogen from the NC ligands. With a sufficient amount of nitrogen atoms around the Co(II) ion, Co(II) can become low spin and its reducing power is drastically increased (stabilisation of the low spin Co(III) state). A very stable Co(III)–NC–Fe(II) pair can then be formed through a chemically-induced electron transfer. Therefore, in order to increase the number of diamagnetic pairs responsible for the photo-induced effect, the number of nitrogen atoms around the cobalt sites has to be increased. When looking at Fig. 1, this is indeed an easy task: it is only required to obtain a Co_1Fe_1 system by introducing alkali cations C(I) in the tetrahedral sites of the framework to get the $C_1Co_1Fe_1$ derivative. Once the diamagnetic pairs are obtained the photo-induced electron transfer should occur, leading to two hypothetical possible excited states: low spin or high spin Co(II)–low spin Fe(III).

In order to understand more deeply the mechanism of the photo-induced electron transfer, we tried to increase the number of diamagnetic pairs in the compounds.

In a first step, Tran Van et al. [64] synthesized two compounds with two opposite stoichiometries: compound **6** $Co(II)_3[Fe(III)(CN)_6]_2 \cdot xH_2O$ or $Co(II)_3Fe(III)_2 \cdot xH_2O$ with a lacunary structure and compound **7** $Cs(I)Co(III)[Fe(II)(CN)_6]$ or $Cs(I)Co(III)_1Fe(II)_1$ close to a *fcc* structure of Co(III) with $[Fe(II)(CN)_6]$ in the octahedral sites and Cs(I) in half of the tetrahedral ones (Fig. 1(c)). From powder diffraction measurements it was discovered that the cell parameter of **7** is smaller by ≈ 0.3 Å than the cell parameter of **6** due to the cobalt change from high spin Co(II) to low spin Co(III). Thanks to the understanding of the role of various synthetic parameters we are now able to synthesize compounds with intermediate stoichiometries such as compound **8** $Rb_{1.8}Co_4[Fe(CN)_6]_{3.30} \cdot 13H_2O$. In this case, the cobalt ligand field appears strong enough to induce a spin change followed by the spontaneous electron transfer from Co(II) to Fe(III). All iron is under the form of $[Fe(II)(CN)_6]$, 80% of the Co–Fe pairs are diamagnetic [Co(III)–Fe(II)], 20% of the pairs are Co(II)–Fe(II) (defect pairs). The structure contains $0.7[Fe(II)(CN)_6]$ vacancies per formula unit, which is a noticeable amount. Compound **6** contains very few diamagnetic pairs, and compound **7** is mainly composed of diamagnetic pairs without vacancies.

In a second step, we studied the conditions of appearance of the photomagnetic effect (Fig. 12). Compound **6**, mainly built from paramagnetic Co(II)–Fe(III) pairs is ferrimagnetic before irradiation with a $T_C \approx 16$ K and no photo-induced change of the magnetisation is observed. Compound **7**, diamagnetic before irradiation, exhibits a very small photomagnetic effect. Compound **8**, essentially diamagnetic before irradiation (with a small amount of paramagnetic Co(II)), exhibits a spectacular photo-induced enhancement of the magnetisation. The comparison of the three results demonstrates that the presence of diamagnetic pairs in the compound is required to observe the photo-induced phenomenon but it is not a

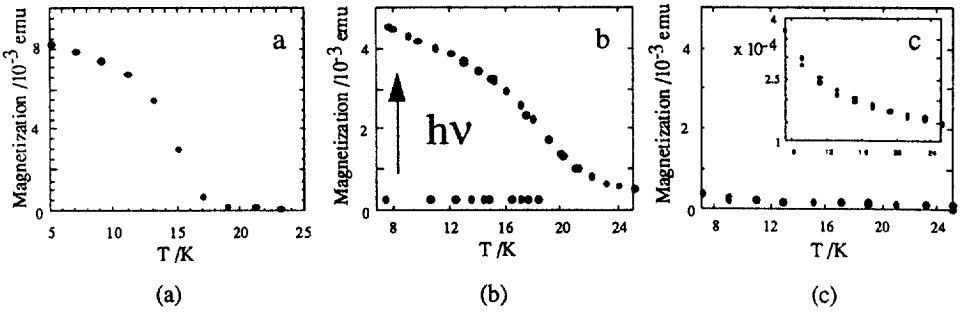

Fig. 12. Magnetisation and photo-induced magnetisation of: (a) compound **6**; (b) compound **8**; and (c) compound **7** (insert: y is scaled $\times$ 10).

sufficient condition [64]. Compound **8** which exhibits the most important photo-induced effect was chosen for the study of the metastable state.

As the first step, we studied the photo-induced magnetic state at the macroscopic and at the microscopic level also. Macroscopically, the photo-excited state was investigated using a SQUID magnetometer equipped with an optical fibre. After photo-excitation in the near IR, compound **8**, mainly built from diamagnetic pairs [Co(III)–Fe(II)] becomes a ferrimagnet with $T_C = 21$ K. The thermal decay of the photo-induced electronic state occurred at 108 K [65]. Microscopically, the electronic structure of the photo-induced magnetic state was investigated by X ray absorption spectroscopy [66]. $L_{2,3}$ edges of 3d transition metals involve symmetry allowed electric dipole transitions from 2p core electrons to incompletely filled 3d and 4s levels. This spectroscopy is particularly suited for oxidation and spin states studies of the metal centres. Our data give, for the first time, clear evidence of the light induced electronic transfer (diamagnetic Co(III)–Fe(II)) → (high spin Co(II)–low spin Fe(III)), first postulated to explain the changes in the macroscopic magnetic properties of the material. The second microscopic characterisation was the investigation of the local structure before and after irradiation by X ray absorption spectroscopy at the Co K edge. The EXAFS data show an increase of the Co–L distance $\Delta d_{Co\ L} = 0.18$ Å induced by irradiation (L is either N(C) or $O(H_2)$. Our studies provide an experimental basis to the explanation of the photo-induced magnetisation first suggested by Sato and coworkers. To the best of our knowledge, this is the first experimental local spectroscopic evidence of a photo-induced metal to metal electron transfer in a three-dimensional compound: [(LS)Co(III)–(LS)Fe(II)] → [(HS)Co(II)–(LS) Fe(III)].

The condition required to observe the phenomenon is not only the presence of diamagnetic excitable pairs (LS)Co(III)–(LS)Fe(II), but also the presence of a certain amount of defects in the cubic structure. This is due to the important expansion of the network accompanying the photo-induced electron transfer. In a perfect structure, without vacancies, strain in the bulk is so strong that only diamagnetic surface pairs are transformed. In a structure with vacancies, the steric constraints are weaker, the network is more flexible and the photo-induced

metastable state is able to propagate in the bulk. We are now engaged in the study of this phenomenon.

4.4. High spin molecules [23–27]

Another brand new direction was opened in cyanide chemistry when our team, in particular Mallah et al. realized 4 years ago that it was possible to get high nuclearity clusters from hexacyanometalates when the Lewis acid opposed to the polycyanide base is not a simple $[A(H_2O)_6]^{n+}$ hexaaqua ion but a complex specially designed to present one (or two) labile positions, $[A(II)L_5(H_2O)_1]$ (L_5 is a pentadentate ligand). Under these conditions, the labile water can be substituted by one cyanide from $[B(CN)_6]$. When the reaction is repeated n times a polynuclear cluster arises since the pentadentate ligand impedes the growing of the three-dimensional Prussian blue phase and the clusters' ground state can present a large spin ($S_{maximum} = 27/2$ up to now in our hands [24,25]). The chemistry is otherwise the same as in Prussian blues and based on the same acid–base Lewis interactions: $[B(III)(CN)_6] + n[A(II)L_5(H_2O)_1] \rightarrow \{[B(III)(CN)_{6-n}](CN-A(II)-L_5)_n\} + nH_2O$

The analysis of the nature of the B–CN–A interaction is essentially the same than in three-dimensional networks since the exchange interactions are short range. The results concerning the nature of the interaction within the clusters are in agreement with the expectations of the model. Such an investigation field is related to the so-called bottom-up approach of nanomagnetism: starting with mononuclear molecular systems with small spins and enhancing the spin borne by each molecule allows to get clean, uniform magnetic objects with high spins to study the reversal of the magnetisation in a magnetic field. The topic is both very fundamental (study of single-molecule magnets, evidence and study of the macroscopic quantum tunneling of the magnetization etc.) and turned to applications (due to a possible huge enhancement of the density of magnetic information per surface unit at the ultimate, molecular scale). We work in two directions: (i) enhancement of the molecular spin; (ii) improvement of the anisotropy of the system since most of the interesting properties are related to the anisotropy barrier, which, in a uniaxial system, is known to be DS_z^2, (D zero-field splitting of the ground spin state). The two requirements (high spin and/or high anisotropy) are often contradictory.

Up to now, we synthesised and fully characterised (by X-ray diffraction on single crystals in the solids and by Electro Spray Mass Spectroscopy in the solutions) a series of trinuclear $\{M(CN)_4[(CN)M'L]_2\}^+$, tetranuclear $\{M(CN)_3[(CN)M'L]_3\}^{3+}$ and heptanuclear $\{M[(CN)M'L]_6\}^{9+}$ complexes. A specific work has been done first on the synthesis of specifically designed tetra- and penta-amine L_4 and L_5 ligands, and their corresponding mononuclear complexes (M(II) = Cu, Ni, Co, Mn). The reaction of $[M(III)(CN)_6]^{3-}$ as a Lewis base with these mononuclear metal ions chelated by L_5 (leaving one labile coordination position only), leads to polynuclear species with a large variety of symmetry induced by the flexibility of the hexa-

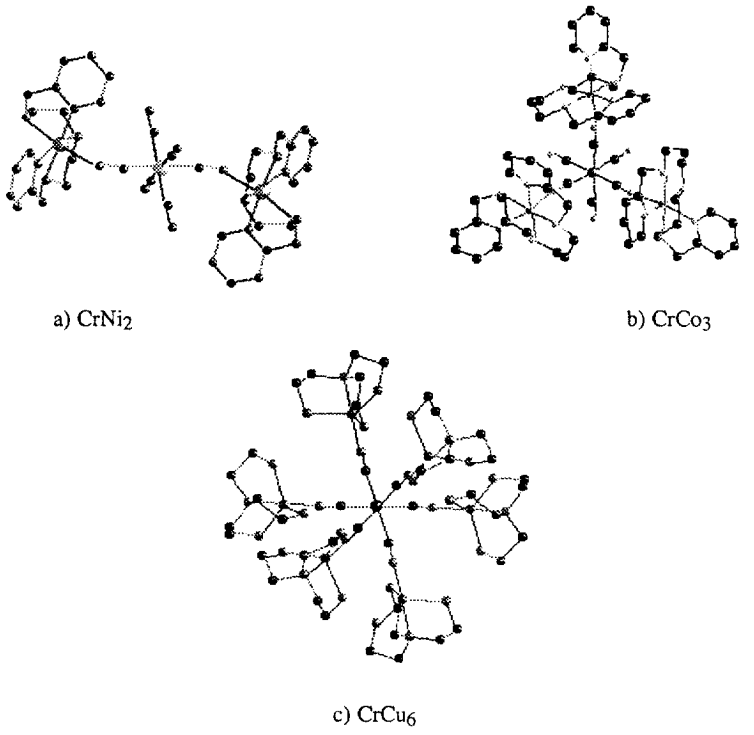

Fig. 13. Perspective view of three polynuclear complexes with different geometry: (a) $CrNi_2$; (b) $CrCo_3$; (c) $CrCu_6$.

cyanometalate coordination chemistry (three structural examples are given in Fig. 13).

The ground state spin value of the molecules can be predicted and tuned according to our model of orbital interactions, by choosing the nature and the number of metallic centers involved. The magnetic measurements have been performed in a SQUID magnetometer on the different complexes: on the one hand, the thermal dependence of the molar susceptibility $\chi_M T = f(T)$, indicates the ferro or antiferromagnetic nature of the interaction; on the other hand, the molar magnetisation as a function of the applied field at $T = 2$ K gives the saturation value corresponding to the spin ground state, S. To evidence and to better understand the nature of the interaction between external metal ions (second neighbour interaction at a distance larger than 10 Å), we also synthesized trinuclear and heptanuclear complexes with a diamagnetic ion at the center [Co(III)]. The main results are reported in Table 2.

To synthesize molecules which present not only a high-spin ground state (either integer or half integer) but also a tunable anisotropy, we are currently (i) carrying out further studies in order to change central and peripheral transition metals and

Table 2
Geometry, symmetry, spin ground state and interaction observed in polynuclear complexes synthesized from [B(III)(CN)$_6$] precursors [B(III) = Cr(III), Co(III)]

Nuclearity	Complex	Geometry	Symmetry	Spin	Interaction[a]
TRI	$CrNi_2$	*Trans*	$D_{\infty h}$	7/2	F
	$CrCo_2$	*Trans*	$D_{\infty h}$	2	AF
	$CoCu_2$	*Cis/trans*	$C_{2v}/D_{\infty h}$	0	af
	$CoNi_2$	*Trans*	$D_{\infty h}$	0	af
TETRA	$CrCo_3$	Facial	C_{3v}	3	AF
HEPTA	$CrCu_6$	Octahedral	O_h	9/2	F
	$CrNi_6$	Octahedral	O_h	15/2	F
	$CrMn_6$	Octahedral	O_h	27/2	AF
	$CoNi_6$	Octahedral	O_h	0	af

[a] F, ferro; AF, antiferro; af, weak antiferromagnetic interaction.

to synthesize lower symmetrical complexes; (ii) trying to better understand how the ground state anisotropy arises from the local ion anisotropies in a given symmetry [67].

If one of the ultimate goals in this field is the synthesis of a single molecule magnet at r.t., we need to fulfill two prerequisites: first, to populate the high spin ground state at r.t., which means an interaction constant between the paramagnetic centres larger than the thermal quantum ≈ 400 K; second, to realize an uniaxial anisotropic barrier $\Delta E_{\text{anisotropy}} = DS_z^2$ of the same order of magnitude i.e. ≈ 400 K, which means for example a total spin $S = 20$ and an anisotropy of the ground state $D = 1$ K. The challenge is difficult but not completely impossible.

5. Conclusion

We tried to show, through different examples essentially chosen in our own chemistry, that exploring old systems with new concepts can give rise to new systems, new properties, and new applications. It was impossible to give in a short text an exhaustive review of all the recent endeavours using hexacyanometalate precursors to build magnetic systems from zero to three dimensions, going through chains and planes. Essentially absent from the review by Felhammer in 1993 [68], these systems have a large place in the 1997 Dunbar's paper 4 years later [69]. The proceedings of the present conference or ICMM'98 are also witnesses to the revival of cyanide chemistry: bimetallic cyanides boxes and superboxes, complex frameworks using less symmetrical precursors than the hexacyano anions, thin layers, photomagnetic and multifunctional systems are appearing or are near completion. We can expect in the near future important and very different achievements in this field, since the flexibility of molecular precursors combines with the versatility of solid state chemistry when molecules build the solid [70].

Acknowledgements

We thank the European Community (Grants ERBCHRXCT92080, ERBFM-BICT972644 and ERBFMRXCT980181) and the European Science Foundation for financial support ('Molecular Magnets' Programme). M.V. is grateful to his former coworkers whose names appear in the references.

References

[1] Anonymous, Miscellanea Berolinensia ad incrementum scientiarum (Berlin) 1 (1710) 377.
[2] H.J. Buser, A. Ludi, W. Petter, D. Schwarzenbach, J. Chem. Soc. Chem. Commun. (1972) 1299.
[3] J.F. Keggin, F.D. Miles, Nature 137 (1936) 577.
[4] A. Ludi, H.U. Güdel, Struct. Bonding 14 (1973) 1.
[5] M.R. Robin, Inorg. Chem. 1 (1970) 337.
[6] A. Ito, M. Suenaga, K. Ono, J. Chem. Phys. 48 (1968) 3597.
[7] D. Gatteschi, O. Kahn, J.S. Miller, F. Palacio (Eds.), Molecular magnetic materials, NATO ASI Series, Series E, vol. 198, Kluwer, Dordrecht, 1991.
[8] V. Gadet, M. Bujoli-Dœuff, L. Force, M. Verdaguer, El Makhi, A. Deroy, J.P. Besse, C. Chappert, P. Veillet, J.P. Renard, P. Beauvillain in Ref. [7], p. 281.
[9] Ref. [7]: see J.S. Miller, p. 151, P. Rey, p. 203, A. Caneshi, p. 215, O. Kahn, p. 35.
[10] J.M. Manriquez, G.T. Yee, R.S. McLean, A.J. Epstein, J.S. Miller, Science 252 (1991) 1415.
[11] M. Verdaguer, V. Gadet, M. Bujoli-Dœuff, T. Mallah, Proceedings of the 13th Conference on Coordination Chemistry, Smolenice, 1991, p. 317.
[12] M. Verdaguer, T. Mallah, V. Gadet, I. Castro, C. Hélary, S. Thiébaut, P. Veillet, in: G. Ondrejovic, A. Sirota (Eds.), Contributions to Development of Coordination Chemistry, Slovak Technical University Press, Bratislava, 1993, p. 19.
[13] C. Roux, C. Hélary, S. Thiébaut, S. Merah, N. Badis, M. Verdaguer, Proceedings of the First European Workshop on Hybrid Organic–Inorganic Materials, Bierville, France, 1993, p. 197.
[14] M. Verdaguer, T. Mallah, S. Ferlay, V. Gadet, C. Hélary, C. Auberger, R. Ouahès, J. Vaissermann, P. Veillet, in: G. Ondrejovic, A. Sirota (Eds.), Current Trends in Coordination Chemistry, Slovak Technical University Press, Bratislava, 1995, p. 291.
[15] T. Mallah, S. Ferlay, C. Auberger, C. Hélary, F. L'Hermite, R. Ouahès, J. Vaissermann, M. Verdaguer, P. Veillet, Mol. Cryst. Liq. Cryst. 273 (1995) 141.
[16] V. Gadet, T. Mallah, I. Castro, P. Veillet, M. Verdaguer, J. Am. Chem. Soc. 114 (1992) 9213.
[17] V. Gadet, Ph.D. Thesis, Université Pierre et Marie Curie, Paris, 1992.
[18] T. Mallah, S. Thiébaut, M. Verdaguer, P. Veillet, Science 262 (1993) 1554.
[19] S. Ferlay, T. Mallah, R. Ouahès, P. Veillet, M. Verdaguer, Nature 378 (1995) 701.
[20] C. Hélary, Ph.D. Thesis, Université Pierre et Marie Curie, Paris, 1996.
[21] S. Ferlay, Ph.D. Thesis, Université Pierre et Marie Curie, Paris, 1996.
[22] E. Dujardin, S. Ferlay, X. Phan, C. Desplanches, C. Cartier dit Moulin, P. Sainctavit, F. Baudelet, E. Dartyge, P. Veillet, M. Verdaguer, J. Am. Chem. Soc. 120 (1998) 11347.
[23] A. Scuiller, Ph.D. Thesis, Université Pierre et Marie Curie, Paris, 1999.
[24] T. Mallah, C. Auberger, M. Verdaguer, P. Veillet, J. Chem. Soc. Chem. Commun. (1995) 61.
[25] A. Scuiller, T. Mallah, A. Nivorozkhin, M. Verdaguer, P. Veillet, New J. Chem. 20 (1996) 1.
[26] S. Ferlay, T. Mallah, J. Vaissermann, F. Bartolomé, P. Veillet, M. Verdaguer, J. Chem. Soc. Chem. Commun. (1996) 2481.
[27] A. Scuiller, V. Marvaud, J. Vaissermann, I. Rosenman, M. Verdaguer, Mol. Cryst. Liq. Cryst. (1999), in press.
[28] A.N. Holden, B.T. Matthias, P.W. Anderson, H.W. Lewis, Phys. Rev. 102 (1956) 1463.
[29] R.M. Bozorth, H.J. Williams, D.E. Walsh, Phys. Rev. 103 (1956) 572.

[30] R. Klenze, B. Kanellopoulos, G. Trageser, H.H. Eysel, J. Chem. Phys. 72 (1980) 5819.
[31] W.D. Griebler, D. Babel, Z. Naturforsch. 87b (1982) 832.
[32] D. Babel, Comments Inorg. Chem. 5 (1986) 285.
[33] L. Néel, Ann. Phys. Paris 3 (1948) 137.
[34] A. Herpin, Théorie du magnétisme, INSTN-PUF, Saclay, 1968.
[35] J.B. Goodenough, Magnetism and the Chemical Bond, Interscience, New York, 1963.
[36] P.J. Haÿ, J.C. Thibeault, R. Hoffmann, J. Am. Chem. Soc. 97 (1975) 4884.
[37] J.J. Girerd, Y. Journeaux, O. Kahn, Chem. Phys. Lett. 82 (1981) 534.
[38] O. Kahn, Molecular Magnetism, VCH, New York, 1993.
[39] M.F. Charlot, O. Kahn, Nouv. J. Chim. 4 (1980) 567.
[40] O. Kahn, Struct. Bonding 68 (1987) 1063.
[41] O. Kahn, Nature 378 (1995) 677.
[42] A. Palii, B. Tsukerblat, T. Mallah, M. Verdaguer, J. Chem. Phys., submitted.
[43] W.R. Entley, G.S. Girolami, Inorg. Chem. 33 (1994) 5165.
[44] W.R. Entley, G.S. Girolami, Science 268 (1995) 397.
[45] W.R. Entley, C.R. Treadway, G.S. Girolami, Mol. Cryst. Liq. Cryst. 273 (1995) 153.
[46] W.R. Entley, C.R. Treadway, S.R. Wilson, G.S. Girolami, J. Am. Chem. Soc. 119 (1997) 6251.
[47] A.J. Epstein, G.S. Girolami, H. Hashimoto, J.S. Miller, Oral Communications at ICMMM'98, Seignosse, France, 12–17 September (1998).
[48] O. Sato, T. Iyoda, A. Fujushima, K. Hashimoto, Science 271 (1996) 49.
[49] W.E. Buschmann, S.C. Paulson. C.M. Wynn, M.A. Girtu, A.J. Epstein, H.S. White, J.S. Miller, Adv. Mater. 9 (1997) 645.
[50] S. Ferlay, T. Mallah, R. Ouahès, P. Veillet, M. Verdaguer, Inorg. Chem., in press.
[51] R. Garde, C. Desplanches, A. Bleuzen, M. Verdaguer, P. Veillet, Mol. Cryst. Liq. Cryst. (1999), in press.
[52] M.A. Arrio, P. Sainctavit, C. Cartier dit Moulin, C. Brouder, F.M.F. De Groot, T. Mallah, M. Verdaguer, J. Phys. Chem. 100 (1996) 4679.
[53] M.A. Arrio, P. Sainctavit, C. Cartier dit Moulin, T. Mallah, M. Verdaguer, E. Pellegrin, C.T. Chen, J. Am. Chem. Soc. 118 (1996) 6422.
[54] M.A. Arrio, P. Sainctavit, C. Cartier, C. Brouder, T. Mallah, M. Verdaguer, J. Phys. IV France, Colloque C2 7 (1997) 409.
[55] G.A.P. Zaldivar, Y. Gushikem, E.V. Benvenutti, S.C. de Castro, A. Vasquez, Electrochim. Acta 39 (1994) 33 and references therein.
[56] W.E. Buschmann, S.C. Paulson, C.M. Wynn, M.A. Girtu, A.J. Epstein, H.S. White, J.S. Miller, Chem. Mater. 10 (1998) 1386.
[57] J.P. Jammet, J. Ferré, J.P. Renard, P. Veillet, P. Beauvillain, C. Train, C. Desplanches, M. Verdaguer, work in progress.
[58] O. Sato, T. Iyoda, A. Fujishima, K. Hashimoto, Science 272 (1996) 704.
[59] M. Verdaguer, Science 272 (1996) 698.
[60] Z.-Z. Gu, O. Sato, T. Iyoda, K. Hashimoto, A. Fujishima, J. Phys. Chem. 100 (1996) 18289.
[61] O. Sato, Z.Z. Gu, H. Etoh, J. Ichiyanagi, T. Iyoda, A. Fujishima, K. Hashimoto, Chem. Lett. 1 (1997) 37.
[62] S.-I. Ohkoshi, O. Sato, T. Iyoda, A. Fujishima, K. Hashimoto, Inorg. Chem. 36 (1997) 268.
[63] O. Sato, Y. Einaga, T. Iyoda, A. Fujishima, K. Hashimoto, J. Electr. Soc. 144 (1997) 11.
[64] P. Tran-Van, P. Veillet, P. Gütlich, J. Ensling, R. Ouahès, M. Verdaguer, C. R. Acad. Sci., submitted.
[65] F. Varret, H. Constant-Machado, J.L. Dormann, A. Goujon, J. Jeftic, M. Noguès, A. Bousseksou, S. Klokishner, A. Dolbecq, M. Verdaguer, ICAME 1997, Rio de Janeiro, Hyperfine interactions 113 (1998) 37.
[66] A. Bleuzen, C. Lomenech, A. Dolbecq, F. Villain, A. Goujon, O. Roubeau, M. Nogues, F. Varret, F. Baudelet, E. Dartyge, C. Giorgetti, J.J. Gallet, C. Cartier dit Moulin, M. Verdaguer, Mol. Cryst. Liq. Cryst. (1999), in press.
[67] B. Tsukerblat, A. Palii, S. Ostrovski, T. Jolicœur, V. Marvaud, M. Verdaguer, work in progress.
[68] W.P. Fehlhammer, M. Fritz, Chem. Rev. 93 (1993) 1243 and references therein.

[69] K. Dunbar, R.A. Heintz, in: K. Karlin (Ed.), Progress Inorg. Chem. 45 (1997) 283 and references therein.

[70] M. Verdaguer, A. Bleuzen, V. Marvaud, J. Vaissermann et al., Coordination Chemistry at the Turn of the Century, G. Oudrejovic, A. Sirota (Eds.), Slovak Technical University Press, Bratislava, 1999, p. 49.